

Self-Assembly of Collagen Fibers. Influence of Fibrillar Alignment and Decorin on Mechanical Properties

George D. Pins, David L. Christiansen, Raj Patel, and Frederick H. Silver

Division of Biomaterials, Department of Pathology and Laboratory Medicine, University of Medicine and Dentistry of New Jersey, and Robert Wood Johnson Medical School, 675 Hoes Lane, Piscataway, New Jersey 08854-5635 USA

ABSTRACT Collagen is the primary structural element in extracellular matrices. In the form of fibers it acts to transmit forces, dissipate energy, and prevent premature mechanical failure in normal tissues. Deformation of collagen fibers involves molecular stretching and slippage, fibrillar slippage, and, ultimately, defibrillation. Our laboratory has developed a process for self-assembly of macroscopic collagen fibers that have structures and mechanical properties similar to rat tail tendon fibers. The purpose of this study is to determine the effects of subfibrillar orientation and decorin incorporation on the mechanical properties of collagen fibers. Self-assembled collagen fibers were stretched 0–50% before cross-linking and then characterized by microscopy and mechanical testing. Results of these studies indicate that fibrillar orientation, packing, and ultimate tensile strength can be increased by stretching. In addition, it is shown that decorin incorporation increases ultimate tensile strength of uncross-linked fibers. Based on the observed results it is hypothesized that decorin facilitates fibrillar slippage during deformation and thereby improves the tensile properties of collagen fibers.

INTRODUCTION

Unmineralized connective tissue functions to maintain shape, transmit and absorb loads, prevent premature mechanical failure, partition cells and tissues into functional units and act as a scaffold that supports tissue architecture (Silver, 1987). The primary structural element in mammalian connective tissue is fibrillar type I collagen. Type I collagen molecules form fibrillar elements, twenty to several hundred nanometers in diameter, which in turn pack into fibril bundles or fibers, fascicles, and higher level tissue architectures (see Birk et al., 1991). The structural hierarchy and mechanical properties of fibrillar type I collagen vary from tissue to tissue; however, the ultimate tensile strength of tissues containing type I collagen has been correlated with fibril (Parry, 1988) and fiber diameters (Doillon et al., 1985).

During loading, collagen molecules, fibrils, and fibril bundles deform and finally fail by a process termed defibrillation (Torp et al., 1975; Folkhard et al., 1987; Sasaki and Odajima, 1996). The exact mechanism by which mechanical energy is translated into molecular and fibrillar deformation is still unclear; however, up to a macroscopic deformation of ~2% molecular stretching predominates (Sasaki and Odajima, 1996). Beyond 2%, increases in the D-period are a result of molecular slippage (Folkhard et al., 1987; Sasaki and Odajima, 1996). The exact magnitude of the strain at which molecular deformation of the triple helix

becomes small compared to molecular and fibrillar slippage depends on the strain rate and tissue studied; however, it is becoming clear that lateral interactions between fibrils are an important aspect of collagen mechanical behavior.

With the exception of collagen, another highly prevalent macromolecule in connective tissue is decorin, a small interstitial dermatan sulfate proteoglycan. Decorin is regularly and specifically associated with the surface of fibrillar type I collagen in extracellular matrices (Scott, 1984). It has been hypothesized that decorin limits collagen fibril diameters by inhibiting the lateral fusion of fibrils (Scott and Orford, 1981; Scott and Parry, 1992; Vogel and Trotter, 1987) and inhibits the mineralization of fibrillar collagen matrices (Scott and Orford, 1981; Scott and Haigh, 1985). Decorin filaments appear to connect adjacent collagen fibrils and therefore it has been proposed that they play a role in maintaining the mechanical integrity of aligned, fibrillar connective tissue (Vogel, 1993; Cribb and Scott, 1995). Despite inferential data, the precise mechanical role of decorin in soft connective tissue has yet to be determined (Vogel, 1993).

Our laboratory has studied the process of collagen self-assembly at the molecular (Silver et al., 1979; Silver and Trelstad, 1979, 1980), fibrillar (Brokaw et al., 1985; Farber et al., 1986), and fibrous levels of structure (Kato et al., 1989; Wang et al., 1994; Pins et al., 1997). At the molecular level, type I collagen assembly involves linear and lateral growth steps that lead to the formation of fibrils with diameters of ~1.2 μm (Brokaw et al., 1985). At the macroscopic level, self-assembled collagen fibers have wet diameters of ~100 μm (Kato et al., 1989) and mechanical properties similar to rat tail tendon fibers (Kato et al., 1989; Wang et al., 1994; Pins et al., 1997). These studies have shown the similarity between the structure and mechanical properties of native and self-assembled fibers. By using this model we are able to study how changes in collagen fibril

Received for publication 28 February 1997 and in final form 2 July 1997.

Address reprint requests to Frederick H. Silver, Biomaterials, V-14, UMDNJ-Robert Wood Johnson Medical School, 675 Hoes Lane, Piscataway, NJ 08854-5635. Tel.: 908-235-4027; Fax: 908-235-4825; E-mail: silverfr@umdnj.edu.

Dr. Pins' present address is Shriners Burns Institute Research Center, One Kendall Square, Cambridge, MA 02139.

© 1997 by the Biophysical Society

0006-3495/97/10/2164/09 \$2.00

structure and interactions with surrounding matrix elements affect mechanical properties. In this paper we report the results of a study to determine the effects of fibrillar orientation and decorin incorporation on the mechanical properties of collagen fibers.

MATERIALS AND METHODS

Isolation and purification of starting materials

Acid-soluble type I collagen (SOL) was obtained from rat tail tendon from Sprague-Dawley rats weighing between 250 and 350 g using a protocol identical to that described by Silver and Trelstad (1980). Collagen was dissolved in 10 mM HCl for 4 h at room temperature, centrifuged at $30,000 \times g$ at 4°C for 30 min, and then serially filtered through 0.65 and 0.45 μm filters (Millipore Corp., Bedford, MA). Type I collagen was isolated by adding NaCl to 0.7 M, then the precipitate was collected by centrifugation ($30,000 \times g$, 4°C, 60 min) and redissolved in 10 mM HCl. Acid-soluble collagen was further purified by dialysis against an aqueous phosphate buffer (20 mM disodium hydrogen phosphate, pH 7.4) overnight at 4°C and the precipitated collagen was collected by centrifugation ($30,000 \times g$, 4°C, 60 min) and dissolved into a concentrated solution by dialyzing the pellets against a large volume of 10 mM HCl overnight at room temperature. The collagen concentration was determined by measuring the absorbance at 230 nm and adjusted to 10 mg/ml (1% w/v) with 10 mM HCl. Collagen solution was stored at 4°C in 30 ml syringes until it was needed for experimentation.

Purity was determined by SDS-PAGE based on the method of Laemmli (1970) and amino acid analysis as described previously (Silver and Trelstad, 1980). The proteoglycan and glycosaminoglycan content in the SOL collagen was determined by uronic acid analysis (Bitter and Muir, 1962). Intrinsic viscosity was conducted to determine the polymeric distribution of collagen molecules in SOL collagen samples. Viscosity measurements were made with a Cannon Ubbelohde viscometer model 0B (State College, PA) maintained at a constant temperature of 20°C. The Simha shape factor (ν) and the average axial ratio (Z) of the molecular collagen aggregates in the starting material were calculated from the Simha equations for the intrinsic viscosity and shape factor of a prolate ellipsoid (Silver, 1987).

Decorin samples were generously donated by Drs. Choi and Rosenberg from the Orthopedic Research Laboratories, Montefiore Medical Center (Bronx, NY). The samples were isolated from fetal bovine skin using the protocol described by Choi et al. (1989). Analyses of these samples indicated that the small dermatan sulfate proteoglycan was composed of a core protein with a single glycosaminoglycan (GAG) chain attached. The decorin ranged from 103 to 120 kD and contained 11% uronic acid (Choi et al., 1989).

Rat tail tendon (RTT) collagen fibers 3–4 cm in length were isolated from the tails of Sprague-Dawley rats by dissection under a microscope. Tendon fibers were split repeatedly along their axes under a microscope until the fibers were $\sim 50 \mu\text{m}$ in diameter. RTT fibers were air dried overnight by hanging the free ends over glass coverslips.

Production of self-assembled collagen fibers

Collagen fibers were self-assembled from SOL collagen using a coextrusion process employing a Micromedics Applicator Tip (Eagan, MN) which consisted of a dual bore (20 ga. \times 2 in.) needle attached to FEP tubing (fluorinated ethylene propylene copolymer, ID 1.27 mm) (See Fig. 1).

The individual bores, fitted with Luer lock connectors, enable the simultaneous extrusion of the contents of two separate syringes. In this system, one of the 5-ml syringes contained a 1% w/v solution of SOL collagen and the other syringe contained a fiber formation buffer (FFB: 135 mM NaCl 30 mM TrizmaBase (Tris), and 5 mM sodium phosphate dibasic, pH 7.4 (Sigma Chemical Co., St. Louis, MO)). With the aid of a syringe pump (Sage Instruments, Cambridge, MA), the two solutions were simultaneously extruded through the FEP tubing into a bath of FFB maintained

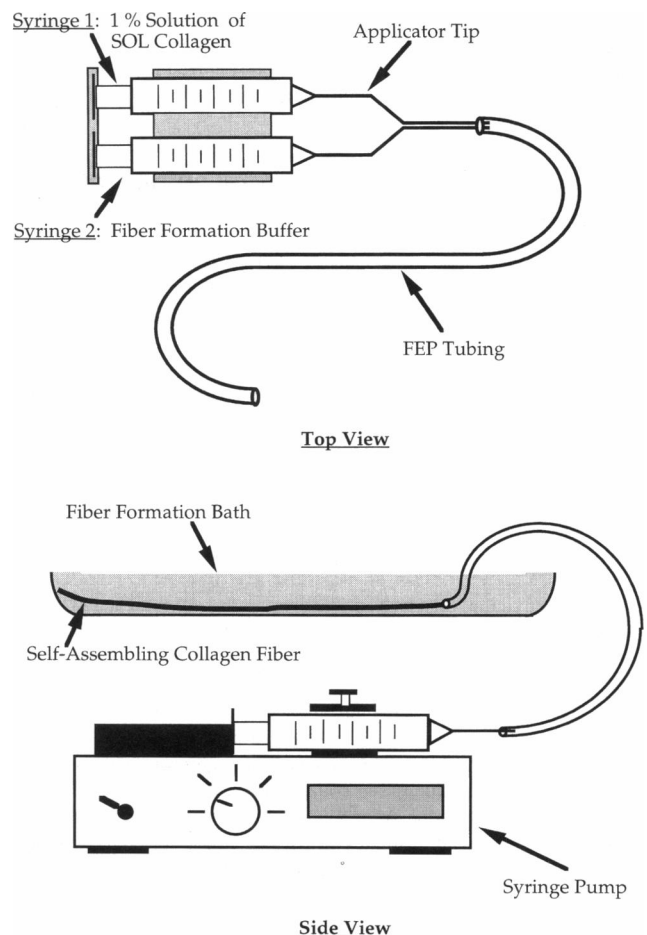


FIGURE 1 Dual syringe extrusion system for producing self-assembled collagen fibers.

at 37°C. After allowing the coextruded fibers to self-assemble in FFB for 24 h, the buffer was aspirated from the bath and replaced with a fiber incubation buffer (FIB: 135 mM NaCl, 10 mM Tris, 30 mM sodium phosphate dibasic, pH 7.4). Fibers were immersed in FIB maintained at 37°C for 24 h, rinsed in distilled water for 60 min, and then air dried under tension (Pins et al., 1997).

Self-assembled collagen fibers (SCF) were subject to static axial stretching using the protocol described previously (Pins et al., 1997). Briefly, collagen fibers attached to a stretching rack were immersed in FIB and then stretched 0, 10, 20, 30, 40, or 50% of their original length. The fibers were maintained at the stretched length for 24 h in FIB at 37°C then removed from FIB and air dried on the rack at their stretched length.

Self-assembled collagen/decorin (SC/DF) fibers were produced by a coextrusion process similar to that described above. In this system, one of the two 5-ml syringes contained a 1% w/v solution of SOL collagen, and the other syringe contained a mixture of 2 \times concentration FFB (pH 7.9) and decorin (300 $\mu\text{g}/\text{ml}$ of FFB) warmed to 37°C. With the aid of a syringe pump, the two solutions were coextruded into a 75-cm length of FEP tubing which was clamped at both ends as the solutions reached the end of the tubing. The clamped tubes were placed in FFB maintained at 37°C for 24 h. After 24 h, the FEP tubes were unclamped and the fibers were extruded from the tubes into a FIB bath by gently flushing the tubes with a syringe containing FIB. The fibers were immersed in FIB bath at 37°C for 24 h then rinsed in distilled water for 60 min and air dried under tension. Self-assembled collagen/control (SC/CF) fibers were produced by omitting decorin from the syringe containing 2 \times concentration FFB. Finally, SC/CF and SC/DF fibers were stretched 0 or 50% using the static axial stretching procedures described above.

Stretched SCF were cross-linked by severe dehydration under conditions previously shown to maximize their ultimate tensile strengths (Wang et al., 1994). Briefly, air dried fibers were cross-linked in a vacuum oven at a pressure of 50–100 mTorr and at a temperature of 110°C for 120 h.

Morphological and ultrastructural studies of collagen fibers

To prepare uncross-linked, stretched, SCF for transmission electron microscopy (TEM), fibers were bundled together with suture and rehydrated in PBS for 60 min. The fibers were subsequently fixed (1.5% glutaraldehyde, 4% formaldehyde, 0.1 M cacodylate, 4 mM CaCl₂, pH 7.4), for 90 min, rinsed in cacodylate buffer, postfixed with osmium tetroxide, and strained en bloc in 2% uranyl acetate (50% ethanol). After serial ethanol dehydration and propylene oxide infiltration, the fiber bundles were embedded in Spurr Epoxy (Ted Pella, Inc., Redding, CA). Thin sections were obtained by cutting either parallel (longitudinal) or perpendicular (transverse) to the long axis of the SCF. Grids were negatively stained with 3% uranyl acetate and 2.0% lead citrate, carbon coated, and viewed with a JEOL 1200 EX electron microscope operated at an accelerating voltage of 80 kV.

The ultrastructural properties of the uncross-linked, stretched SCF were quantitated using image analysis techniques. The negatives were subsequently enlarged to a final magnification of approximately 81,000× and two randomly chosen square regions, each representing a 500 nm × 500 nm area of collagen fiber, were outlined on each micrograph. For each fiber type, 2.0 μm² of fiber area were analyzed. Outlined regions of micrographs were scanned into a Macintosh II computer equipped with an Apple Scanner (300 dpi resolution) and collagen fibril areas (*A*) and perimeters (*P*) within a square region of a micrograph were measured by particle analysis using National Institutes of Health Image v1.60/ppc program (developed at the US National Institutes of Health). Collagen fibril diameters (*f_d*) were calculated from the measured cross-sectional areas using the equation $f_d = 2[\text{sqrt}(A/\pi)]$. The aligned fibril area fraction for each fiber type was calculated as the total fibril area per total fiber area measured. The shape factor (*S*) was used to quantitatively assess the shape of the fibrils in the transverse plane of the fibers. The shape factor ($S = 4A\pi/P$) is a measure of circularity where *S* is 1 for a perfect circle and zero for a straight line (McBride et al., 1988).

To localize decorin, uncross-linked fibers were prepared for TEM analysis using the protocol described by Scott and Orford (1981). Bundles of fibers were rehydrated in PBS then fixed and stained for 18 h in a Cuprolinic Blue solution (2.5% glutaraldehyde, 300 mM MgCl₂, 25 mM sodium acetate, and 0.05% Cuprolinic Blue (Polysciences, Inc., Warrington, PA)). Samples were rinsed in fixative minus the stain and then water, stained en bloc with 0.5% sodium tungstate solution, dehydrated with a graded ethanol series, infiltrated with propylene oxide, and embedded in Spurr Epoxy (Ted Pella, Inc., Redding, CA). Thin sections were obtained by cutting both parallel (longitudinal) and perpendicular (transverse) to the long axis of the collagen fibers. Grids were double stained for collagen with 3% uranyl acetate and 1% phosphotungstic acid solution (pH 7.4). Carbon coated grids, both stained and unstained, were viewed with a JEOL 1200 EX electron microscope at an accelerating voltage of 80 kV.

Volumetric analyses of stretched SCF were made by approximating the mean fiber volumes as circular cylinders. The lengths of the fibers were measured after static axial stretching and the mean cross-sectional areas of the fibers were determined after rehydration with a Leitz Pol microscope (Rockleigh, NJ) fitted with a calibrated eyepiece.

Birefringence retardation measurements

Semi-thin (3 μm), longitudinal sections of embedded (JB-4, Polysciences, Warrington, Pa.) cross-linked, stretched SCF were examined with polarizing optics and monochromatic light as described previously (Pins et al., 1997) to determine birefringence retardation. Before each birefringence measurement, sections were immersed in water (*n* = 1.333) for at least 90

min. Unstained sections were evaluated using a Leitz 12 Pol microscope fitted with a monochrome filter ($\lambda = 546$ nm) and a Leitz Brace-Kohler $\lambda/10$ calibrated compensator as previously described (McBride et al., 1988). For each type of fiber analyzed, six measurements were made on randomly selected regions. Birefringence retardation values were normalized by dividing by the fiber thickness.

Tensile mechanical testing of collagen fibers

Uniaxial tensile tests were conducted on fibers using the protocol previously described (Kato et al., 1989). Stretched, cross-linked fibers were mounted on paper frames with a gauge length of 20 mm. The mounted fibers were immersed in PBS for 60 min prior to testing. The approximate cross-sectional areas of the fibers were determined before (dry) and after rehydration (wet) using a Leitz Pol microscope (Rockleigh, NJ) fitted with a calibrated eyepiece. The fibers were then mounted in the grips of an Instron Model 1122 Tensile Tester (Instron Corp., Canton, MA), the edges of the frame were cut and a tensile load was applied to the fibers at a constant deformation rate of 10 mm/min. From the resulting load/deformation curves and the measured diameters of the fibers, the ultimate tensile strengths (UTS), strains at failure, and tangent moduli for the fibers were determined.

Uronic acid analysis of collagen/decorin fibers

The decorin content of the self-assembled collagen/decorin fibers was determined by the uronic acid assay using the uronate method (Bitter and Muir, 1962). Measured quantities of self-assembled collagen/decorin fiber and self-assembled collagen/control fiber stretched 0 or 50% were treated with carbazole for uronic acid analysis. The optical densities of the resulting solutions were measured and the uronic acid content of each solution was extrapolated from a standard calibration curve for D-glucuronic acid. The difference in uronic acid content between collagen/decorin and collagen/control fibers was used to calculate the amount of decorin in the fibers by assuming that the decorin was composed of 11% uronic acid.

Statistical analyses

Statistical comparisons between sample groups were made using an analysis of variance (ANOVA) with *p* ≤ 0.05 indicating a significant difference between mean values. Post hoc comparisons between two sample groups in a pool were made with Fisher's PLSD (protected least significant difference) analysis with *p* ≤ 0.05 indicating a significant difference between mean values.

Statistical comparisons between SC/CF and SC/DF fibers analyzed for uronic acid content were evaluated using a one-tailed Student's *t*-test with *p* ≤ 0.05 indicating a significant difference between mean values.

RESULTS

Purity and compositional analyses of SOL collagen

Based on gel electrophoresis, after reduction and heat denaturation, the SOL collagen was determined to be type I collagen, composed primarily of α chains, β and γ components, in addition to a small quantity of high molecular weight aggregates. Amino acid analyses were also typical of type I collagen. The noncollagenous proteoglycan and glycosaminoglycan content of the SOL collagen was determined to be <0.1% (w/w) based on uronic acid analysis. Intrinsic viscosity measurements were made to determine the polymeric distribution of the collagen molecules in the

SOL collagen starting material. Based on previous observations that acid-extracted tendon collagen was primarily composed of monomeric and 4-D staggered dimeric collagen (Silver and Trelstad, 1980; Fleischmajer et al., 1991), the SOL collagen was calculated to be 73% monomeric and 27% 4-D staggered dimers.

Morphological and ultrastructural properties of SCF

The 1% (w/v) solution of SOL collagen, from which the SCF were made, appeared clear and slightly viscous. When the collagen solution was extruded into fiber formation buffer, the fiber slowly developed into a visible thread. The appearance of the SCF did not change during the 48-h fiber formation process. The gross morphology of SCF was not visibly altered by static axial stretching or cross-linking.

The fibrillar substructure and organization of SCF were characterized by analyzing longitudinal and transverse sections with a transmission electron microscope after sections were double-stained with uranyl acetate and lead citrate (see Fig. 2). A transverse section of an SCF-0% fiber (Fig. 2 *a*) shows cross-sections of collagen fibrils indicating axial orientation as well as fibrils oriented perpendicular to the long axial of SCF-0%. Fig. 2 *d* shows a micrograph of a section cut longitudinally with respect to the long axis of an uncross-linked SCF stretched 0% (SCF-0%). It indicates that the matrix contains collagen fibrils which exhibit D-periodic banding patterns comparable to those observed in native collagen fibrils, but demonstrate only partial orien-

tation with respect to the long axis of the fiber. The presence of cross-sections of collagen fibrils also indicates that the fibrils are oriented obliquely with respect to the long axis of the fiber. The micrograph of a section cut longitudinally to the long axis of an uncross-linked SCF stretched 30% (SCF-30%) (Fig. 2 *e*) indicates the presence of collagen fibrils with D-periodic banding patterns. When compared with the fibrils in the SCF-0% fiber, Fig. 2 *d*, the fibrils in the SCF-30% matrix appear to have a higher degree of orientation with respect to the long axis of the scaffold. A small number of obliquely oriented collagen fibrils were also noted in the longitudinal section. Transverse sections of SCF-30% (Fig. 2 *b*) show a predominance of cross-sections of collagen fibrils. This confirmed that SCF stretched 30% was primarily composed of axially oriented collagen fibrils with only a few collagen fibrils oriented obliquely with respect to the long axis of the fiber. Transmission electron micrographs of uncross-linked SCF stretched 50% (SCF-50%) are shown in Figs. 2 *c* and *f*. A transverse section of SCF-50%, Fig. 2 *c*, confirmed that the fiber was composed of densely packed collagen fibrils that were oriented parallel to the long axis of the fiber. The micrograph of a section cut parallel to the long axis of the SCF-50% (Fig. 2 *f*) indicates the presence of D periodically banded collagen fibrils that are highly oriented with respect to the long axis of the SCF-50%.

The mean collagen fibril diameters and aligned fibril area fractions were calculated and are summarized in Table 1. The mean collagen fibril diameters of stretched collagen fibers exhibited only nominal variation. The mean fibril diameter for fibers stretched 50% was significantly greater than for fibers stretched 0, 10, 20, 30, and 40%. Fibers stretched 40% had fibril diameters that were significantly less than all other groups tested. All of the stretched SCF exhibited a broad, unimodal distribution of fibril diameters. The aligned fibril area fraction also varied as SCF was stretched. The total fiber area composed of axially aligned collagen fibrils increased considerably when SCF matrices were stretched at least 30%. The greatest aligned fibril area fraction was observed in SCF matrices stretched 50%. The shape factor showed little variation as SCF was stretched, but the values indicated that the fibrils within each matrix type were not circular.

Qualitative volumetric analyses based on mean diameters of rehydrated fibers were used to investigate the effect of static axial stretching on the lateral contraction of uncross-linked SCF. The results of these calculations indicated that the mean volumes of self-assembled fibers decreased as the fibers were stretched. This decrease in volume indicates that the lateral contraction of the uncross-linked SCF increased as the extent of stretching increased.

Form birefringence measurements were made on semi-thin sections of cross-linked collagen fibers to quantitate the degree of ordered aggregation of fibrils. Analyses of measurements on cross-linked collagen fibers indicated that SCF stretched at least 30% had form birefringence values comparable to RTT and significantly greater than fibers

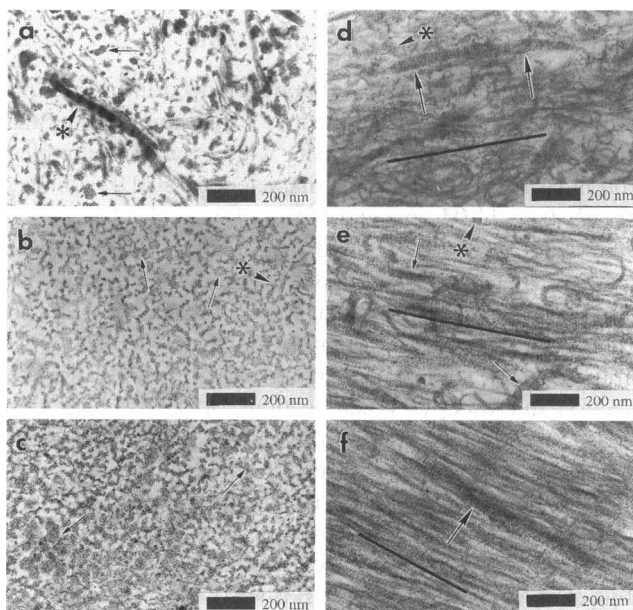


FIGURE 2 Transmission electron micrographs of self-assembled collagen fibers stretched 0%, 30%, and 50% (SCF-0%). Transverse (*a-c*) and longitudinal (*d-f*) views of SCF-0% (*a, d*), SCF-30% (*b, e*), and 50% (*c, f*) fibers. Note the increased orientation of fibers stretched 50% (*f*) compared to 0% (*d*). Arrows point to individual collagen fibrils and asterisks indicate fibril cross-sections.

TABLE 1 Morphological properties of stretched, uncrosslinked, self-assembled collagen fibers (SCF)

Fiber Type	Fibril Areas Measured	Aligned Fibril Area Fraction	Mean Fibril Diameter (nm)	Shape Factor
SCF-0%	426	0.117	24.15 ± 10.71	0.890 ± 0.0435
SCF-10%	316	0.0787	23.62 ± 8.74	0.880 ± 0.0478
SCF-20%	335	0.0758	22.48 ± 8.44	0.896 ± 0.0434
SCF-30%	713	0.181	23.10 ± 10.66	0.900 ± 0.0393
SCF-40%	686	0.155	19.47 ± 8.78*	0.908 ± 0.0449
SCF-50%	867	0.231	26.47 ± 12.60*	0.888 ± 0.0431

Aligned fibril area fraction = sum of axially aligned fibril area (nm²) divided by total area measured (μm²). Mean values given as average ± standard deviation.

* Significantly different from SCF-0%.

stretched up to 20%. Additionally, fiber stretched 30% exhibited form birefringence values that were significantly higher than comparable fiber stretched 40% (Fig. 3). Fibers stretched >20% had birefringence retardation values statistically similar to the values reported for RTT.

Mechanical properties of cross-linked SCF

The mechanical properties of cross-linked SCF were determined by loading the matrices in uniaxial tension until failure. These values, as well as the mechanical properties of native RTT, are summarized in Table 2. Analyses of UTS indicated that SCF stretched at least 20% before cross-linking had values that were comparable to RTT and significantly greater than fibers stretched 0 or 10% (Fig. 4). There was no significant difference between the UTS values of fibers stretched 20, 30, 40, or 50%. The strain at failure values of SCF fibers that were stretched 20, 30, 40, or 50% were comparable to each other and to RTT. The tangent

modulus values of SCF fibers stretched at least 20% before cross-linking were comparable to RTT and significantly higher than SCF fibers stretched 0 or 10%. SCF stretched between 30 and 50% had tangent modulus values that were comparable to each other and significantly greater than fibers stretched 20%. The load-at-failure values of the cross-linked SC/CF fibers did not vary significantly with stretching. RTT fibers had load-at-failure values that were significantly greater than all SCF fibers. Wet diameter values of SCF fibers stretched between 20 and 50% before cross-linking were not significantly different from each other, although fibers stretched at least 20% had wet diameters that were significantly smaller than fibers stretched 0 or 10%. RTT had wet diameters that were significantly greater than any of the SCF fibers. SCF stretched 20% had dry diameters that were similar to SCF fibers stretched 30 or 40%, but significantly greater than SCF fibers stretched 50%.

Morphological properties of SC/DF

The fibrillar substructure and collagen/decorin interactions within SCF were characterized by examining longitudinal and transverse sections of fibers with a transmission electron microscope. Mean fibril diameters of SC/DF stretched 0% (24.6 ± 11.04 nm) and 50% (23.9 ± 11.42 nm) were significantly greater than the diameters of 0% (22.5 ± 9.23) and 50% (21.8 ± 10.24 nm) stretched SCF fibers. The presence of decorin in collagen/decorin fibers was confirmed by staining SC/CF and SC/DF with the GAG-specific dye Cuprolicin Blue during sample preparation for electron microscopy. When sections of these fibers were viewed in an electron microscope without additional staining, the GAG chains of the decorin molecules were readily noted within the fibers. To ensure that the GAG chains observed in the SC/DF fibers were not the result of residual impurities from the collagen extraction process, Cuprolicin Blue-stained sections of SC/DF fibers were compared with similarly prepared sections of SC/CF fibers. Only trace quantities of GAG chains were detected in SC/CF fibers. The GAG chains of the decorin molecules in the Cuprolicin Blue-stained sections had mean lengths of 44.7 ± 8.37 nm (*n* = 12). Using a conversion factor of 500 Da/nm, (Scott et al., 1990), the GAG chains were calculated to be ~22,350 Da.

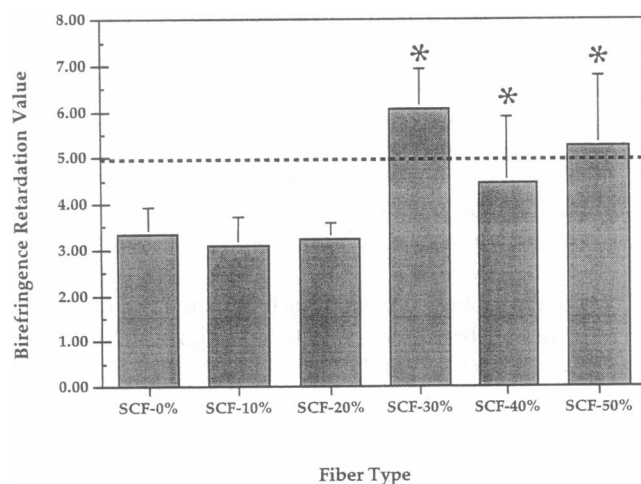


FIGURE 3 Birefringence retardation values ($G/t \times 10^3$) for cross-linked collagen fibers. Optical retardation measurements (G) were made on semi-thin sections (thickness, t) of self-assembled collagen fibers (SCF), which were rehydrated in PBS for 60 min and then stretched 0, 10, 20, 30, 40, or 50% before cross-linking. The birefringence retardation value for native rat tail tendon is denoted by the dashed black line. Values of birefringence retardation that are statistically greater than that of fibers stretched 0% (SCF-0%) are denoted with an asterisk.

TABLE 2 Results of uniaxial tensile tests for cross-linked collagen fibers

Fiber Type (<i>n</i>)	UTS (MPa)	Strain (%)	Tangent Modulus (MPa)	Load (g)	Wet Diameter (μm)	Dry Diameter (μm)
SCF-0% (19)	38.44 \pm 13.30	19.03 \pm 2.45	252.4 \pm 71.52	35.34 \pm 6.66	111.5 \pm 22.99	74.00 \pm 11.38
SCF-10% (17)	40.44 \pm 13.11	16.51 \pm 2.40	304.2 \pm 85.75	37.93 \pm 8.15	111.6 \pm 20.66	74.30 \pm 11.23
SCF-20% (23)	54.46 \pm 13.18*	14.68 \pm 2.31*	432.9 \pm 82.09*	38.14 \pm 11.36	94.35 \pm 16.15*	64.30 \pm 9.95*
SCF-30% (21)	57.10 \pm 11.82*	13.80 \pm 1.68*	503.9 \pm 101.1*	43.88 \pm 12.63	98.95 \pm 19.50*	66.20 \pm 12.54*
SCF-40% (20)	55.16 \pm 12.11*	13.18 \pm 2.85*	528.7 \pm 99.84*	36.17 \pm 8.81	90.65 \pm 9.33*	58.75 \pm 5.01*
SCF-50% (18)	56.62 \pm 11.17*	13.15 \pm 1.63*	539.1 \pm 53.69*	35.85 \pm 9.01	88.72 \pm 8.57*	55.5 \pm 5.17*
RTT (7)	53.5 \pm 11.10*	13.9 \pm 1.90*	498.8 \pm 44.0*	268.6 \pm 84.4	250.3 \pm 38.4*	

SCF-X % = self-assembled collagen fibers stretched 0–50%; RTT = rat tail tendon fibers. All fibers were tested in uniaxial tension at a strain rate of 10 mm/min after rehydrating the fibers for 60 min in PBS. All values given as mean \pm standard deviation; *n* = number of samples.

* Statistically different from SCF-0%.

Sections of Cuprolic Blue-stained SC/DF fibers were also positively stained with uranyl acetate and phosphotungstic acid to characterize the location of the decorin within the collagen fibrils. Self-assembled collagen/decorin fibers stretched 0% (SC/DF-0%) are shown in Fig. 5, *a* and *c*. A longitudinal section stained only with Cuprolic Blue (Fig. 5 *a*) shows the presence of single, small groups, and large clusters of decorin distributed throughout the fiber. Longitudinal sections of SC/DF-0% fiber stained with uranyl acetate and phosphotungstic acid revealed collagen fibril organization and collagen/decorin interactions (Fig. 5 *c*). Collagen/decorin interactions were noted at the d bands of the collagen fibrils, but interactions were observed at other fibril bands as well. Additionally, clusters of decorin were noted in regions between collagen fibrils.

Transmission electron micrographs of SC/DF stretched 50% (SC/DF-50%) are shown in Fig. 5, *b* and *d*. A longitudinal section of a fiber stained only with Cuprolic Blue (Fig. 5 *b*) indicates the presence of single and small groups of decorin molecules within the SC/DF-50% fiber. Collagen

fibril organization and collagen/decorin interactions were investigated by staining longitudinal sections of SC/DF-50% fiber with uranyl acetate and phosphotungstic acid (Fig. 5 *d*). GAG filaments of decorin molecules were associated with the surface of collagen fibrils and exhibit various orientations, but many are oriented axially or orthogonally with respect to the collagen fibrils. Collagen/decorin interactions were noted at the d bands of the collagen fibrils, but interactions were observed at other fibril bands as well. In regions between adjacent collagen fibrils, some GAG chains appear to be attached to neighboring fibrils.

Uronic acid analysis of SC/DF

The decorin content of the SC/DF was determined using the uronic acid assay. The results of the uronic acid analysis shown in Table 3 indicate that the SC/DF fibers stretched 0% contain significantly more uronic acid than SC/CF fibers stretched 0%. The difference in uronic acid content

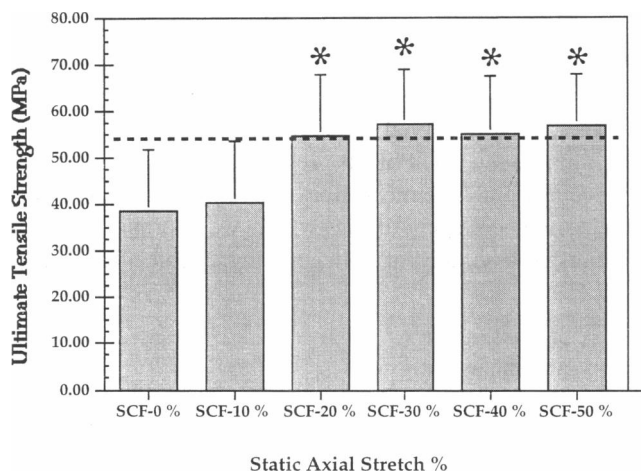


FIGURE 4 Ultimate tensile strengths of cross-linked, self-assembled collagen fibers. Matrices were rehydrated in PBS for 60 min and then loaded in uniaxial tension until failure. SCF-X% = self-assembled collagen fibers stretched 0–50% and the dashed line represents rat tail tendon (RTT). Values of ultimate tensile strength that are statistically greater than those of fibers stretched 0% (SCF-0%) are denoted with an asterisk.

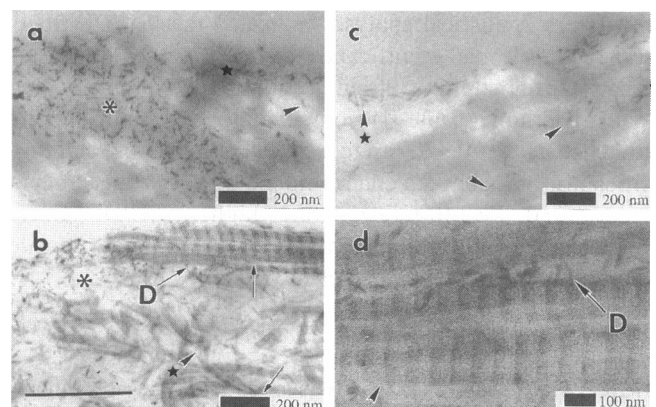


FIGURE 5 Transmission electron micrographs of self-assembled collagen/decorin fibers stretched 0% and 50%. (*a*) (0% stretch) and (*c*) (50% stretch) illustrate a longitudinal section of fibers stained only with Cuprolic Blue. (*b*) (0% stretch) and (*d*) (50% stretch) show fibers stained with uranyl acetate and phosphotungstic acid and reveal collagen fibril organization and collagen/decorin interactions. In (*b*) and (*d*) D represents decorin associated with the collagen fibril banding pattern. In (*a*) and (*c*) the asterisk and star show regions of high decorin staining. All arrows and arrowheads indicate association between decorin and collagen fibrils.

TABLE 3 Results of uronic acid analysis of collagen samples

Sample Type	Sample Weight (mg)	Average Absorb.	Uronic Acid Content (μg)*	Normalized Uronic Acid Content ($\mu\text{g}/\text{mg}$)	Average Normalized Uronic Acid Content ($\mu\text{g}/\text{mg}$)
SC/CF-0%	6.70	0.098	5.03	0.751	0.723 \pm 0.040
SC/CF-0%	6.05	0.090	4.20	0.694	
SC/CF-50%	4.08	0.064	1.60	0.392	0.609 \pm 0.306
SC/CF-50%	3.23	0.075	2.67	0.826	
SC/DF-0%	6.67	0.140	9.23	1.384	1.468 \pm 0.119 [#]
SC/DF-0%	5.96	0.141	9.25	1.552	
SC/DF-50%	3.70	0.088	3.97	1.072	0.985 \pm 0.123
SC/DF-50%	3.49	0.079	3.13	0.898	

SC/CF-X% = self-assembled collagen/control fiber stretched 0 or 50%. SC/DF-X% = self-assembled collagen/decorin fiber stretched 0 or 50%. Average values reported as mean \pm standard deviation.

* Uronic acid values extrapolated from standard calibration curve.

[#] Statistically different from SC/CF-0%.

between the two fiber types indicates that the SC/DF fibers stretched 0% contain 6.77 μg of decorin/mg of collagen. The uronic acid content of SC/DF fibers stretched 50% was not significantly different from the uronic acid content of SC/CF control fibers stretched 50%, but SC/DF fibers stretched 50% contained significantly less uronic acid than SC/DF fibers stretched 0%. The difference in uronic acid content between SC/DF fibers stretched 50 and 0% indicates that SC/DF fibers stretched 50% contain \sim 2.38 μg of decorin/mg of collagen. SC/CF control fibers stretched 0 and 50% had uronic acid content values that were comparable to each other and to the SOL collagen starting material.

Mechanical properties of collagen/decorin fibers

Uniaxial tensile tests were conducted to determine the effect of decorin incorporation on mechanical properties of collagen fibers. Statistical analyses indicated that SC/DF fibers stretched 50% had significantly different values of the ultimate tensile strength, strain at failure, swelling ratio, and load at failure (Table 4) compared to SC control fibers stretched 50%. At 0% stretch, SC/DF fibers were not significantly stronger than control fibers; however, the strain at failure and load-to-failure were higher. SC/DF fibers stretched 50% had higher values of the ultimate tensile strength compared to unstretched fibers.

DISCUSSION

It has been known since the 1950s that microscopic collagen fibrils that exhibit D periodic banding patterns characteristic of those seen in connective tissue will self-assemble in vitro from solutions of collagen molecules (Gross et al., 1952; Jackson and Fessler, 1955). Recently, we have been able to self-assemble collagen in the form of fibers that have sub-fibrillar structure that mimics that seen in tissues in vivo (Pins et al., 1997). The utility of this system is that the mechanical properties of fibers with different substructures can be assessed. In this study we evaluated the effects of fibril alignment and incorporation of decorin on the mechanical properties of D-periodic collagen fibers.

The collagen fibril diameters reported in this study averaged between 20 and 26 nm with unimodal diameter distributions that are significantly less than those observed in mature tendons (Kastelic et al., 1978; Rowe, 1985; Torp et al., 1975; Parry and Craig, 1977), but they are comparable to those observed by Torp et al. (1975) in tail tendon of newborn rats and by Birk et al. (1990) in chick embryo tendon at 10 days of development. This correlation suggests that the fibrils observed in self-assembled collagen fibers are similar to the small fibrils present during the early stages of development. The mean fibril diameters are also similar to the small collagen fibrils, which were proposed to be products of assembly of collagen single molecules in pre-

TABLE 4 Results of uniaxial tensile tests for self-assembled collagen/decorin fibers

Fiber Type (n)	UTS (MPa)	% Strain	Tangent Modulus (MPa)	Load (g)	Wet Diameter (μm)	Swelling Ratio
SC/CF-0% (34)	0.772 \pm 0.459	47.8 \pm 7.92	2.32 \pm 1.24	5.34 \pm 2.52	309.1 \pm 42.8	3.217 \pm 0.529
SC/DF-0% (42)	1.359 \pm 1.019	54.8 \pm 13.2	4.50 \pm 6.23	8.23 \pm 2.34*	296.1 \pm 53.8	2.669 \pm 0.476
SC/CF-50% (37)	3.500 \pm 2.255*	26.1 \pm 6.06*	16.2 \pm 10.3*	9.74 \pm 4.64*	200.8 \pm 40.7	2.449 \pm 0.544
SC/DF-50% (49)	4.643 \pm 2.340*	31.3 \pm 7.37*	19.1 \pm 12.2*	11.5 \pm 4.63*	190.5 \pm 47.9	2.227 \pm 0.370*

SC/CF-X% = self-assembled collagen/control fiber stretched 0 or 50%. SC/DF-X% = self-assembled collagen/decorin fiber stretched 0 or 50%. All fibers were tested in uniaxial tension at a strain rate of 10 mm/min after rehydrating the fibers for 60 min in PBS. All values given as mean \pm standard deviation; (n) = number of samples.

* Statistically different from SC/CF-0%.

vious reports (Silver and Trelstad, 1979, 1980). The similarities between small fibrils formed microscopically (Silver and Trelstad, 1979, 1980) and the larger scale collagen fibers formed here suggest that the mechanisms are likely the same. These findings also parallel the results of *in vivo* assembly in tendon reported by Birk and Zycband (1994), suggesting that the product of the *in vitro* model approximates that which forms *in vivo*.

To evaluate the effect of fibrillar alignment on mechanical properties, collagen fibers were stretched between 0 and 50%. The results of uniaxial tests confirmed that the mechanical properties of SCF were changed by static axial stretching. SCF stretched by at least 30% before cross-linking exhibited ultimate tensile strengths, strains at failure, and moduli comparable with rat tail tendon fibers. Computational analyses and aligned fibril area fractions quantitatively indicated that there were increases in fibril orientation when SCF were stretched 30–50%.

These results suggest that there is a parallel between self-assembly, alignment, and compaction of collagen fibrils *in vitro* and the formation of aligned collagen fibrils *in vivo*. The question next arises as to how tension is applied to collagen fibrils during the self-assembly process *in vivo*. It is well known that the cell cytoskeleton is linked via integrins to extracellular matrix collagen (Hynes, 1987; Staatz et al., 1991). In addition, during fibrillogenesis *in vivo* it has been observed that collagen fibrils are seen within invaginations in the cell membrane (Trelstad and Hayashi, 1979). Furthermore, *in vivo* it has been reported that fibroblasts provide tension during wound contraction (Watts et al., 1958) and *in vitro* that they can contract collagen lattices (Bell et al., 1979). Therefore, it seems possible that collagen fibril alignment *in vivo* may be achieved via cytoskeletal-induced forces at points at which collagen fibrils are being added to fibers within the deep invaginations in the cell membrane. Furthermore, from our *in vitro* results it may be inferred that stretching induces increased fibrillar orientation and packing density perhaps via increased numbers of interactions between amino acid residues on the surface of collagen molecules. The findings parallel the works of Vilarta and de Campos Vidal (1989) and de Campos Vidal and de Carvalho (1990), which suggested that the improved tensile strength of collagen fibers results from increased fibrillar alignment and packing density, leading to increased “strong interactions within or between collagen fibrils” (de Campos Vidal and de Carvalho, 1990).

Once collagen fibers were produced composed of collagen fibrils similar to those seen in developing tissues, we were then able to study the effect of addition of decorin. Surprisingly, even the presence of a small amount of decorin was easily observed by EM in unaligned collagen fibers, and the resulting collagen fibers had increased load-to-failure. Even more surprising was the fact that stretching collagen fibers containing decorin by 50% appeared to lead to decreased amounts of decorin; however, even after dissociation these collagen fibers had improved ultimate ten-

sile strengths compared to unstretched fibers containing decorin. SC/DF fibers stretched 0% that underwent a similar incubation procedure contained more decorin than SC/DF fibers stretched 50%. Although the amount of decorin measured using the uronic acid analysis is only semi-quantitative, the results indicate that even small amounts of decorin affect mechanical properties. The amount of decorin incorporated in this study was ~10% of the saturation amount reported by Brown and Vogel (1989).

The above results suggest that decorin-type I collagen interactions appear to be stable in the absence of tensile stretching and improve the load to failure of collagen fibers. However, in the presence of tensile loads, many of the collagen-decorin interactions are broken and the decorin diffuses away, at least *in vitro*. Hypothetically, loss of decorin from collagen-decorin fibers suggests that decorin may not only be involved in increasing the tensile strength of collagen fibrils *in vivo* but also act as a regulatory signal that is released when large tensile loads are being borne by collagen fibers. Release of decorin may be a signal to local collagen-producing cells to increase collagen deposition to help support the load. The stretch-induced loss of decorin from collagen fibrils may promote increased lateral interactions between collagen fibrils, which would effectively increase the fibril diameter and result in increased tensile strength of collagen fibrils and fibers (Doillon et al., 1985; Parry, 1988). A recent paper proposed that decorin is a bidentate ligand that attaches to two parallel neighboring collagen molecules in the fibril helping to stabilize fibrils and orient them during fibrillogenesis (Scott, 1996). A modification of this model might include a role for decorin in aligning collagen molecules and fibrils during tensile loading.

A question that needs to be addressed is regarding how decorin would increase the tensile strength of collagen fibrils and fibers. Considering that the shear stiffness of proteoglycan aggregates has been estimated to be only 10^{-5} MPa (Mow et al., 1984), it is likely that the presence of proteoglycans only indirectly affects the mechanical properties. Since collagen molecular and fibrillar slippage plays an important role in the tensile deformation of aligned connective tissue such as tendon (Folkhard et al., 1987; Sasaki and Odajima, 1996), it is more likely that decorin plays a role in promoting either molecular or collagen fibrillar slippage. The increased tensile strength of the collagen-decorin fiber stretched 50% compared to the stretched fiber without decorin or the unstretched fiber with decorin implies that the role of decorin, at least in these *in vitro* studies, is to promote collagen fibril alignment, which would facilitate collagen fibrillar slippage and improve lateral interactions during tensile deformations.

In contrast, in tissues with large amounts of aggregating proteoglycans (aggrecan) such as articular cartilage, proteoglycans theoretically behave quite differently, since stress-induced compression drives dehydration of the extracellular matrix, inducing collapse of the proteoglycan molecules and an increased resistance to further compression. Collapse of

the proteoglycan molecules and charge repulsion might also lead to increased electrostatic interactions of proteoglycans with collagen, and in this case inhibit collagen fibrillar slippage.

REFERENCES

- Bell, E., B. Ivarsson, and C. Merrill. 1979. Production of a tissue-like structure by contraction of collagen lattices by human fibroblasts of different proliferative potential in vitro. *Proc. Natl. Acad. Sci. USA*. 76:1274-1278.
- Birk, D. E., F. H. Silver, and R. L. Trelstad. 1991. Matrix assembly. In *The Cell Biology of the Extracellular Matrix*, 2nd Ed., E. D. Hay, editor. Academic Press, New York. 221-254.
- Birk, D. E., and E. I. Zycband. 1994. Assembly of the tendon extracellular matrix during development. *J. Anat.* 184:457-463.
- Birk, D. E., E. I. Zycband, D. A. Winkelman, and R. L. Trelstad. 1990. Collagen fibrillogenesis in situ. *Ann. N.Y. Acad. Sci.* 580:176-194.
- Bitter, T., and H. M. Muir. 1962. A modified uronic acid carbazole reaction. *Anal. Biochem.* 4:330-334.
- Brokaw, J. L., C. J. Doillon, R. A. Hahn, D. E. Birk, and F. H. Silver. 1985. Turbidimetric and morphological studies of type I collagen fibre self assembly in vitro and the influence of fibronectin. *Int. J. Biol. Macromol.* 7:135-140.
- Brown, D. C., and K. G. Vogel. 1989. Characteristics of the in vitro interaction of a small proteoglycan (PG II) of bovine tendon with type I collagen. *Matrix.* 9:468-478.
- Choi, H. U., T. L. Johnson, S. Pal, L.-H. Tang, L. Rosenberg, and P. J. Neame. 1989. Characterization of the dermatan sulfate proteoglycans, DS-PGI and DS-PGII, from bovine articular cartilage and skin isolated by octyl-Sepharose chromatography. *J. Biol. Chem.* 264:2876-2884.
- Cribb, A. M., and J. E. Scott. 1995. Tendon response to tensile stress: an ultrastructural investigation of collagen-proteoglycan interactions in stressed tendon. *J. Anat.* 187:423-428.
- de Campos Vidal, B., and H. F. de Carvalho. 1990. Aggregational state and molecular order of tendons as a function of age. *Matrix.* 10:48-57.
- Doillon, C. J., M. G. Dunn, E. Bender, and F. H. Silver. 1985. Collagen fiber formation in vivo: development of wound strength and toughness. *Coll. Relat. Res.* 5:481-492.
- Farber, S., A. K. Garg, D. E. Birk, and F. H. Silver. 1986. Collagen fibrillogenesis in vitro: evidence for pre-nucleation and nucleation steps. *Int. J. Biol. Macromol.* 8:37-42.
- Fleischmajer, R., J. S. Perlsh, and T. Faraggiana. 1991. Rotary shadowing of collagen monomers, oligomers and fibrils during tendon fibrillogenesis. *J. Histochem. Cytochem.* 19:51-58.
- Folkhard, W., E. Mosler, W. Geercken, E. Knorzer, H. Nemetschek-Gansler, Th. Nemetschek, and M. H. J. Koch. 1987. Quantitative analysis of the molecular sliding mechanism in native tendon collagen-time-resolved dynamic studies using synchrotron radiation. *Int. J. Biol. Macromol.* 9:169-175.
- Gross, J., J. H. Highberger, and F. O. Schmitt. 1952. Some factors involved in the fibrogenesis of collagen in vitro. *Proc. Soc. Exp. Biol. Med.* 80:462-465.
- Hynes, R. O. 1987. Integrins: a family of cell surface receptors. *Cell.* 48:549-554.
- Jackson, D. S., and J. H. Fessler. 1955. Isolation and properties of a collagen soluble in salt solution at neutral pH. *Nature.* 176:69-70.
- Kastelic, J., A. Galeski, and E. Baer. 1978. The multicomposite structure of tendon. *Connect. Tissue Res.* 6:11-23.
- Kato, Y. P., D. L. Christiansen, R. A. Hahn, S.-J. Shieh, J. D. Goldstein, and F. H. Silver. 1989. Mechanical properties of collagen fibres: a comparison of reconstituted and rat tail tendon fibres. *Biomaterials.* 10:38-42.
- Laemmli, U. K. 1970. Cleavage of structural proteins during the assembly of the head of bacteriophage T4. *Nature.* 227:680-685.
- McBride, D. J., Jr., R. L. Trelstad, and F. H. Silver. 1988. Structural and mechanical assessment of developing chick tendon. *Int. J. Biol. Macromol.* 10:194-200.
- Mow, V. C., A. F. Mak, W. M. Lai, L. C. Rosenberg, and L.-H. Tang. 1984. Viscoelastic properties of proteoglycan solutions with varying proportions present as aggregates. *J. Biomech.* 17:325-338.
- Parry, D. A. D. 1988. The molecular and fibrillar structure of collagen and its relationship to mechanical properties of connective tissue. *Biophys. Chem.* 29:195-209.
- Parry, D. A. D., and A. S. Craig. 1977. Quantitative electron microscope observations of the collagen fibrils in rat-tail tendon. *Biopolymers.* 16:1015-1031.
- Pins, G. D., E. K. Wang, D. L. Christiansen, and F. H. Silver. 1997. Effects of axial strain on the tensile properties and failure mechanisms of collagen fibers. *J. Appl. Polym. Sci.* 63:1429-1440.
- Rowe, R. W. D. 1985. The structure of rat tail tendon fascicles. *Connect. Tissue Res.* 14:21-30.
- Sasaki, N., and S. Odajima. 1996. Elongation mechanism of collagen fibrils and force-strain relationships of tendon at each level of structural hierarchy. *J. Biomech.* 9:1131-1136.
- Scott, J. E. 1984. The periphery of the developing collagen fibril. *Biochem. J.* 218:229-233.
- Scott, J. E. 1996. Proteodermatan and proteokeratan sulfate (decorin, lumican/fibromodulin) proteins are horseshoe shaped. Implications for their interactions with collagen. *Biochemistry.* 35:8795-8797.
- Scott, J. E., C. Cummings, H. Greiling, H. W. Stuhlsatz, J. D. Gregory, and S. P. Damle. 1990. Examination of corneal proteoglycans and glycosaminoglycans by rotary shadowing and electron microscopy. *Int. J. Biol. Macromol.* 12:180-184.
- Scott, J. E., and M. Haigh. 1985. Proteoglycan-type I collagen fibril interactions in bone and non-calcifying connective tissues. *Biosci. Rep.* 5:71-81.
- Scott, J. E., and C. R. Orford. 1981. Dermatan sulfate-rich proteoglycan associates with rat tail-tendon collagen at the d band in the gap region. *Biochem. J.* 197:213-216.
- Scott, J. E., and D. A. D. Parry. 1992. Control of collagen fibril diameters in tissues. *Int. J. Biol. Macromol.* 14:292-293.
- Silver, F. H. 1987. *Biological Materials: Structure, Mechanical Properties and Modeling of Soft Tissues*. New York University Press, New York. 91-110.
- Silver, F. H., K. H. Langley, and R. L. Trelstad. 1979. Type I collagen fibrillogenesis: initiation via reversible linear and lateral growth steps. *Biopolymers.* 18:2523-2535.
- Silver, F. H., and R. L. Trelstad. 1979. Linear aggregation and the turbidimetric lag phase: type I collagen fibrillogenesis in vitro. *J. Theor. Biol.* 81:515-526.
- Silver, F. H., and R. L. Trelstad. 1980. Type I collagen in solution: structure and properties of fibril fragments. *J. Biol. Chem.* 255:9427-9433.
- Staatz, W. D., K. F. Fok, M. M. Zutter, S. P. Adams, B. A. Rodriguez, and S. A. Santoro. 1991. Identification of a tetrapeptide recognition sequence for the $\alpha 2(\text{I})$ integrin in collagen. *J. Biol. Chem.* 266:7363-7367.
- Torp, S., E. Baer, and B. Friedman. 1975. Effects of age and of mechanical deformation on the ultrastructure of tendon. In *Structure of Fibrous Biopolymers*, Coston papers No. 26, E. D. T. Atkins and A. Keller, editors. Butterworths, London. 223-250.
- Trelstad, R. L., and K. Hayashi. 1979. Tendon collagen fibrillogenesis: intracellular subassemblies and cell surface changes associated with fibril growth. *Dev. Biol.* 71:228-242.
- Vilarta, R., and B. de Campos Vidal. 1989. Anisotropic and biomechanical properties of tendons modified by exercise and denervation: aggregation and macromolecular order in collagen bundles. *Matrix.* 9:55-61.
- Vogel, K. G. 1993. Glycosaminoglycans and proteoglycans. In *Extracellular Matrix Assembly and Structure*, P. D. Yurchenco, D. E. Birk, and R. P. Mecham, editors. Academic Press, San Diego. 243-280.
- Vogel, K. G., and J. A. Trotter. 1987. The Effect of proteoglycans on the morphology of collagen fibrils formed in vitro. *Coll. Relat. Res.* 7:105-114.
- Wang, M.-C., G. D. Pins, and F. H. Silver. 1994. Collagen fibers with improved strength for the repair of soft tissue injuries. *Biomaterials.* 15:507-512.
- Watts, G. T., H. C. Grillo, and J. Gross. 1958. Studies in wound healing. II. The role of granulation tissue in contraction. *Ann. Surg.* 148:153-160.